



Electrochemical Properties of $0.3\text{Li}_2\text{MnO}_3 \cdot 0.7\text{LiMn}_{0.55}\text{Ni}_{0.30}\text{Co}_{0.15}\text{O}_2$ Electrode Containing VGCF for Lithium Ion Battery

Jeong-Min Kim¹, Minchan Jeong², Bong-Soo Jin², and Hyun-Soo Kim^{2,*}

¹LG Chem, Daejeon 305-738, Korea

²Korea Electrotechnology Research Institute, Changwon 641-120, Korea

Abstract : The $0.3\text{Li}_2\text{MnO}_3 \cdot 0.7\text{LiMn}_{0.55}\text{Ni}_{0.30}\text{Co}_{0.15}\text{O}_2$ cathode material was prepared via a co-precipitation method. The vapor grown carbon fiber (VGCF) was used as a conductive material and its effects on electrochemical properties of the $0.3\text{Li}_2\text{MnO}_3 \cdot 0.7\text{LiMn}_{0.55}\text{Ni}_{0.30}\text{Co}_{0.15}\text{O}_2$ cathode material were investigated. From the XRD pattern, the typical complex layered structure was confirmed and a solid solution between Li_2MnO_3 and LiMO_2 ($M = \text{Ni}, \text{Co}$ and Mn) was formed without any secondary phases. The VGCF was properly distributed between cathode materials and conductive sources by a FE-SEM. In voltage profiles, the electrode with VGCF showed higher discharge capacity than the pristine electrode. At a 5C rate, 146 mAh/g was obtained compared with 232 mAh/g at initial discharge in the electrode with VGCF. Furthermore, the impedance of the electrode with VGCF did not changed much around 9-10 Ω while the pristine electrode increased from 21.5 Ω to 46.3 Ω after the 30th charge/discharge cycling.

Keywords : energy storage materials, lithium ion battery, chemical synthesis, electrochemistry, X-ray diffraction

Received December 26, 2013 : Accepted February 7, 2014

1. Introduction

Recently, Lithium ion batteries have been widely investigated due to the demands for high energy density, power and safety in large-scale applications such as PHEV, HEV, EV and energy storage systems. LiCoO_2 cathode material has commercialized dominantly thus far, because it has good productivity and cycling performance. Co, however, as one of the base materials, is expensive and highly toxicity. Furthermore, LiCoO_2 shows relatively low thermal stability and discharge capacity, which are essential in new cathode materials for the next generation lithium ion batteries.

Therefore, many different kinds of cathode materials have been examined extensively in the last decade

such as Li_2MnO_3 , LiFePO_4 , $\text{LiCo}_x\text{Ni}_{1-x}\text{O}_2$, $\text{LiNi}_x\text{Mn}_y\text{Co}_{(1-x-y)}\text{O}_2$, etc. to replace LiCoO_2 .¹⁻⁵⁾ Among those materials, $\text{LiNi}_x\text{Mn}_y\text{Co}_{(1-x-y)}\text{O}_2$, generally referred to as NCM, has been reported to enhance thermal stability and electrochemical properties by substituting transition metals (Mn, Ni or Al) in LiCoO_2 for Co.³⁾ Especially, the solid solution created by Li_2MnO_3 and LiMO_2 ($M = \text{Mn}, \text{Ni}$ and Co), a complex layered compound, is considered to be promising cathode material because of its high reversible capacity of about 230-250 mAh/g when it is charged up to 4.8 V vs Li^+/Li , and its structural stability attributed to electrochemically inactive Mn^{4+} ions during charge and discharge.⁶⁻¹⁰⁾ On the other hand, as the content of Mn ions increase, discharge capacity considerably decreases at a high current rate because of the high internal resistance in the electrode caused by the Jahn-Teller distortion, due to the Mn^{3+} ions.^{8,10)} Therefore, one of the most crucial factors in order to improve the electrochemical properties of lithium ion

*Corresponding author. Tel.: +82 55 280 1699

E-mail address: hskim@keri.re.kr

batteries is to minimize the internal resistance.

As a step toward improving the electric conductivity of the $0.3\text{Li}_2\text{MnO}_3 \cdot 0.7\text{LiMn}_{0.55}\text{Ni}_{0.30}\text{Co}_{0.15}\text{O}_2$ cathode material, VGCF was chosen in this study based on the previous result as a conductive material. It was reported that VGCF connected among particles and decreased the internal resistance.¹¹⁾ Therefore, it is possible to assume that VGCF could facilitate the Li ion and electron migration among particles.

In this aspect, the effects of the VGCF as a conductive material on $0.3\text{Li}_2\text{MnO}_3 \cdot 0.7\text{LiMn}_{0.55}\text{Ni}_{0.30}\text{Co}_{0.15}\text{O}_2$ cathode material were investigated in terms of its electrochemical performances in this study.

2. Experimental

The metal precursors of $0.3\text{Li}_2\text{MnO}_3 \cdot 0.7\text{LiMn}_{0.55}\text{Ni}_{0.30}\text{Co}_{0.15}\text{O}_2$ cathode material were prepared via a co-precipitation method using $\text{MnSO}_4 \cdot \text{H}_2\text{O}$, $\text{NiSO}_4 \cdot 6\text{H}_2\text{O}$, and $\text{CoSO}_4 \cdot 7\text{H}_2\text{O}$ as starting materials. At the same time, NaOH and NH_4OH as chelating agents were fed into the reactor in appropriate amounts and pH was maintained in the range of 11-11.5 during the process.¹²⁾ After co-precipitation, (Ni, Co, Mn)(OH)₂ precursors were filtered, washed five times by distilled water, and then dried at 100°C for 24 h. Subsequently, the powder with stoichiometric $\text{LiOH} \cdot \text{H}_2\text{O}$ was thoroughly mixed and annealed at 900°C for 3 h in air.

In order to fabricate the electrode, a cathode material, super pure black (SPB) as conductive materials, and poly vinylidene fluoride (PVDF) as a binder, were slurried with *n*-methyl pyrrolidone (NMP) solvent in the ratio of 84:8:8 (wt %). To compare the effects of VGCF, an electrode with 3 wt % VGCF was also produced in the ratio of 84:5:3:8 (wt %). The slurry after blending was coated on an aluminum current collector foil and dried at 100°C for 12 h.

X-ray diffraction analysis was employed to confirm the crystal structure and impurities in the synthesized active material, using an X-pert PW3830 (Philips Co.) with Cu K α radiation under conditions of 40 kV and 30 mA. In addition, a field emission scanning electron microscope (FE-SEM, S-4800, Hitachi Co.) was used to observe the particle size and surface morphology.

For electrochemical measurements, coin-type cells (CR2032 type) consisting of a lithium foil as an anode, a separator (Celguard®3501), and a cathode electrode, ethylene carbonate (EC) / dimethyl ethyl

carbonate (DEC) = 1/1 (vol.%) with dissolved LiPF_6 used as the electrolyte were constructed in a dry room.

The electrochemical performances were measured by a battery cycler (TOCAT-3100, TOYO System). The $0.3\text{Li}_2\text{MnO}_3 \cdot 0.7\text{LiMn}_{0.55}\text{Ni}_{0.30}\text{Co}_{0.15}\text{O}_2$ cathode electrode was charged and discharged in the voltage range of 2.0 - 4.6 V by the constant current (CC) - constant voltage (CV) method. Rate capability was evaluated at current rates of 0.1 C, 1 C, 2 C and 5 C while the cycling performance was tested at a current rate of 1 C at room temperature. EIS was measured for the discharged cell using an IM6 (ZAHNER, Germany) in the frequency range of 1 Hz - 1 MHz at 10 mV of amplitude, and cyclic voltammogram (CV) was operated at 0.1 mV/s between 2.0 V and 4.6 V at room temperature.

3. Results and discussion

The XRD pattern of the co-precipitated $0.3\text{Li}_2\text{MnO}_3 \cdot 0.7\text{LiMn}_{0.55}\text{Ni}_{0.30}\text{Co}_{0.15}\text{O}_2$ cathode material was shown in Fig. 1. The pattern measured in this study was found to well coincide with typically hexagonal $\alpha\text{-NaFeO}_2$ structure and previously reported results as indexed. In addition, (018) and (110) reflections were clearly split and a Li_2MnO_3 -like region around 21-23° was observed, indicating that the complex layered structure between Li_2MnO_3 and $\text{LiMn}_{0.55}\text{Ni}_{0.30}\text{Co}_{0.15}\text{O}_2$ were well formed without any remarkable impurities.⁷⁾

Fig. 2 showed the morphology of the $0.3\text{Li}_2\text{MnO}_3 \cdot 0.7\text{LiMn}_{0.55}\text{Ni}_{0.30}\text{Co}_{0.15}\text{O}_2$ electrode together with its constituent materials observed using the FE-SEM. The average particle size of the cathode material synthesized in this study was approximately 300-500 nm. Fig. 2(a)-(c) represent the $0.3\text{Li}_2\text{MnO}_3$

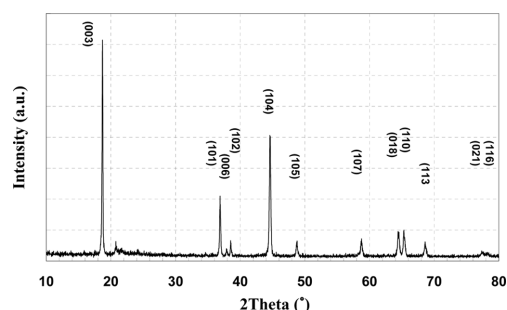


Fig. 1. XRD pattern of the $0.3\text{Li}_2\text{MnO}_3 \cdot 0.7\text{LiMn}_{0.55}\text{Ni}_{0.30}\text{Co}_{0.15}\text{O}_2$ powder.

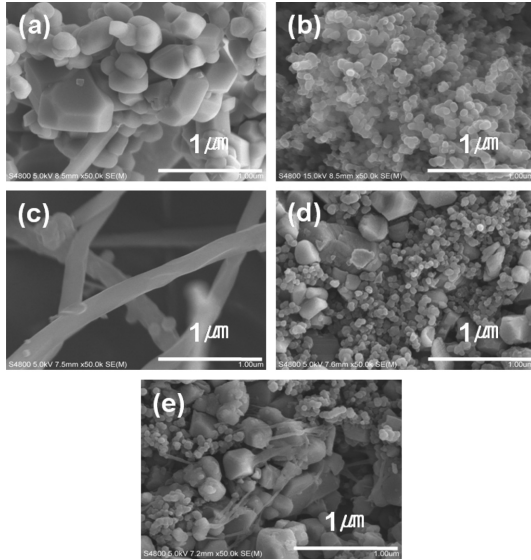


Fig. 2. FE-SEM images of the $0.3\text{Li}_2\text{MnO}_3 \cdot 0.7\text{LiMn}_{0.55}\text{Ni}_{0.30}\text{Co}_{0.15}\text{O}_2$ electrode together with its constituent materials : (a) active material (b) SPB (c) VGCF (d) pristine electrode (e) electrode with 3 wt% VGCF addition.

$\text{O}_3 \cdot 0.7\text{LiMn}_{0.55}\text{Ni}_{0.30}\text{Co}_{0.15}\text{O}_2$ powder, SPB and VGCF, respectively. As presented in Fig. 2(e), VGCF was considered to play the role of the connector between cathode material particles other than the pristine electrode as shown in Fig. 2(d). In other words, VGCF could be expected to improve electric conductivity with other conductive materials, SPB in this study, by providing a path to electrically charged Li ions or electrons.

Fig. 3 provided CV results of the $0.3\text{Li}_2\text{MnO}_3 \cdot 0.7\text{LiMn}_{0.55}\text{Ni}_{0.30}\text{Co}_{0.15}\text{O}_2$ electrode to inspect the reversibility of redox reaction according to the addition of VGCF using fresh samples in the potential range of 2.0-4.6 V. The VGCF made no noticeable difference and no abnormal reactions were observed. The redox peaks around 3.7-4.2 V were attributed to $\text{Ni}^{2+}/\text{Ni}^{4+}$ followed by $\text{Co}^{3+}/\text{Co}^{4+}$ reactions at a higher potential region. Moreover, the decomposition of Li_2MnO_3 to Li_2O and MnO_2 was also found at 4.6 V.

The voltage profiles of the $0.3\text{Li}_2\text{MnO}_3 \cdot 0.7\text{LiMn}_{0.55}\text{Ni}_{0.30}\text{Co}_{0.15}\text{O}_2$ electrode after the first and second charge/discharge cycle were presented in Fig. 4. The initial discharge capacity of electrode with VGCF was nearly 232 mAh/g, compared with 224 mAh/g of the pristine electrode at a current rate of 0.1 C. In the coulombic efficiency, 75.2 % and

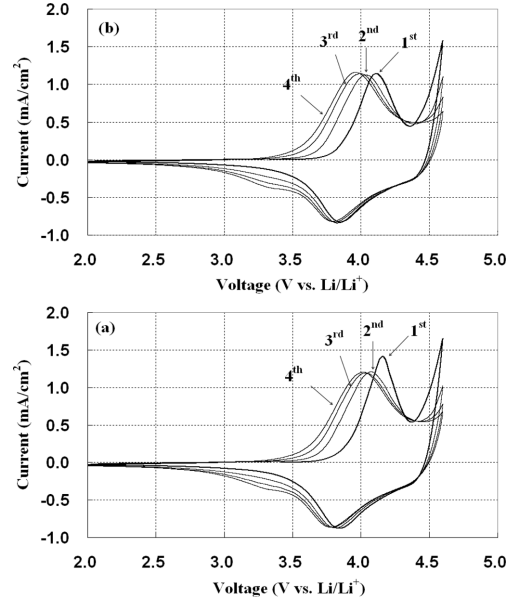


Fig. 3. Cyclic voltammograms of the $\text{Li}/0.3\text{Li}_2\text{MnO}_3 \cdot 0.7\text{LiMn}_{0.55}\text{Ni}_{0.30}\text{Co}_{0.15}\text{O}_2$: (a) pristine (b) electrode with 3 wt% VGCF addition.

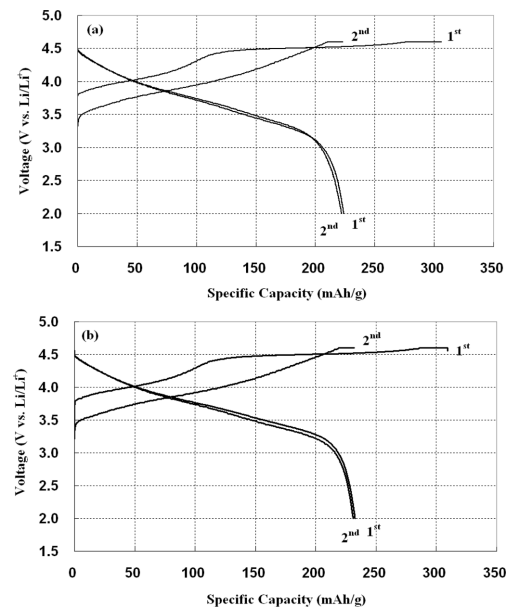


Fig. 4. Charge/discharge voltage profiles of the $\text{Li}/0.3\text{Li}_2\text{MnO}_3 \cdot 0.7\text{LiMn}_{0.55}\text{Ni}_{0.30}\text{Co}_{0.15}\text{O}_2$ cells : (a) pristine (b) 3 wt% VGCF addition.

73.2% were obtained for the electrode with VGCF and the pristine respectively, which resulted from irreversible capacity loss mainly due to the removal

of Li₂O from the Li₂MnO₃ structure. As a result, the discharge capacity was somewhat improved with the VGCF, but the redox reaction region by metal ions did not change much with CV data as described in Fig. 3.

Fig. 5 represented the rate capability of a 0.3Li₂MnO₃·0.7LiMn_{0.55}Ni_{0.30}Co_{0.15}O₂ electrode at current rates of 0.1 C, 1 C, 2 C and 5 C at room temperature. At a low current density of 0.1 C, both electrodes delivered a similar discharge capacity. With an increase in current rate from 1 C to 5 C, however, discharge capacity of the pristine electrode dramatically faded from 179 to 112 mAh/g in contrast to the electrode with VGCF down from 186 to 146 mAh/g. As with the rate capability, the impedance measured in the frequency range of 1 Hz - 1 MHz showed a similar tendency, as shown in Fig. 6. The internal resistance of the electrode with VGCF was 9.4 Ω lower than the pristine, 21.5 Ω. Even after 5th and 30th charge/discharge cycling, the internal resistance did not increased much for the electrode with VGCF, whereas the pristine electrode increased up to 46.3 Ω. Thus, by adding the VGCF as a conductive substance, migration of Li ions could be facilitated through the surfaces of particles when it was charged and discharged in an electrode, resulting in the decreased internal resistance.

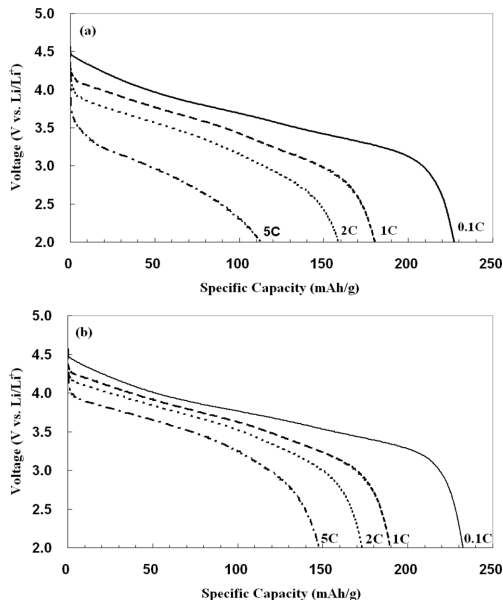


Fig. 5. Rate capability of the Li/0.3Li₂MnO₃·0.7LiMn_{0.55}Ni_{0.30}Co_{0.15}O₂ cells at the 0.1 C, 1 C, 2 C and 5 C rate : (a) pristine (b) 3 wt% VGCF addition.

The electrode with VGCF showed a superior discharge capacity of 173 mAh/g compared to the pristine electrode of about 151 mAh/g and capacity

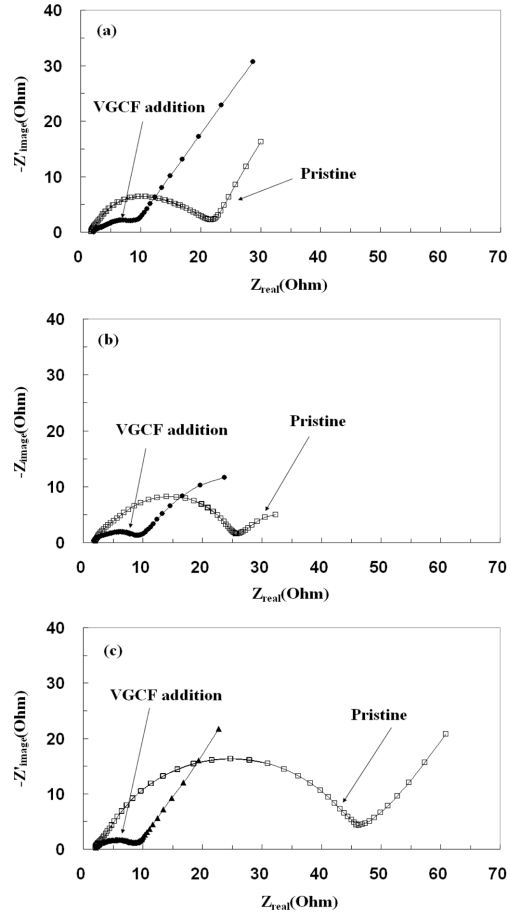


Fig. 6. AC Impedance spectra of the Li/0.3Li₂MnO₃·0.7LiMn_{0.55}Ni_{0.30}Co_{0.15}O₂ cells: (a) after 2nd cycle, (b) after 5th cycle and (c) after 30th cycle.

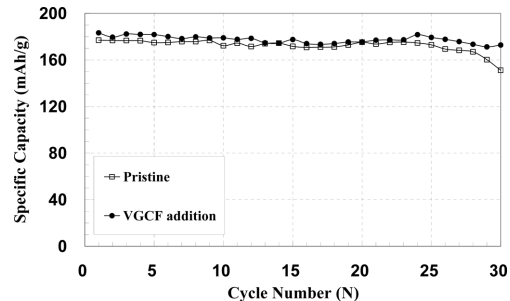


Fig. 7. Cycle-life performances of the Li/0.3Li₂MnO₃·0.7LiMn_{0.55}Ni_{0.30}Co_{0.15}O₂ cells operated between 2.0 and 4.6 V at the 1 C rate : (a) pristine (b) 3 wt% VGCF addition.

retention of 93% and, 85% respectively after the 30th charge/discharge cycling at a 1 C rate in Fig. 7. In comparison with the impedance profiles as shown in Fig. 6, the impedance of the pristine electrode was comparable to the electrode with VGCF after 5th cycles while the impedance of the pristine electrode significantly increased in contrast to those of electrode with VGCF after 30th cycles. Consequently, cycle performance of the pristine electrode showed the tendency to fade dramatically after 25th cycles.

In conclusion, the VGCF enhanced not only rate capability at a high current rate, but also cycle performance by improving the electric conductivity of an electrode.

4. Summary

The 0.3Li₂MnO₃·0.7LiMn_{0.55}Ni_{0.30}Co_{0.15}O₂ cathode material was synthesized using a co-precipitation method. The traditional layered hexagonal α -NaFeO₂ structure was confirmed to be without impurities by an X-ray diffraction. VGCF as a conductive material was well mixed with 0.3Li₂MnO₃·0.7LiMn_{0.55}Ni_{0.30}Co_{0.15}O₂ particles and SPB. In electrochemical tests, the electrode with VGCF showed resistivity lower than the pristine electrode. In addition, 146 mAh/g of discharge capacity was delivered at a current rate of 5 C and 93% of the capacity retention was also obtained in the electrode with VGCF even after the 30th charge/discharge cycling. Consequently, it was suggested in this study that VGCF as a conductive material was effective in improving electrochemical properties including rate capability, impedance, and cycle-life performance, and it provided the passage way to the cathode materials, particularly Li ions and electrons for electric conductivity.

Acknowledgements

This research was supported by a grant from the Energy Technology R&D Programs of the Ministry of Knowledge Economy, Korea (No. 2008-11-0055).

References

1. C.X. Ding, Q.S. Meng, L. Wang and C.H. Chen, *Mater. Res. Bull.*, **44**, 492 (2009).
2. S.J. Jin, C.H. Song, K.S. Park, A.M. Stephan, K.S. Nahm, Y.S. Lee, J.K. Kim and H.T. Chung, *J. Power Sources*, **158**, 620 (2006).
3. K.M. Shaju, G.V. Subba Rao and B.V.R. Chowdari, *Electrochim. Acta.*, **48**, 145 (2002).
4. B.W. Kang and G. Ceder, *Nature.*, **458**, 190 (2009).
5. Y.K. Sun, S.T. Myung, B.C. Park, J. Prakash, I. Belharouak and K. Amine, *Nature Mater.*, **8**, 320 (2009).
6. Francis A, Daniela K, Michael T, Leila Z, Judith G, Nicole L, Gil G, Boris M and Doron A, *J. Electrochem. Soc.*, **157**, 1121 (2010).
7. M.M. Thackeray, C.S. Johnson, J.T. Vaughey, N. Li and S.A. Hackney, *J. Mater. Chem.*, **15**, 2257 (2005).
8. X.J. Guo, Y.X. Li, M. Zheng, J.M. Zheng, J. Li, Z.L. Gong and Y. Yang, *J. Power Sources*, **184**, 414 (2008).
9. M.M. Thackeray, S.H. Kang and C.S. Johnson, J.T. Vaughey, S and A. Hackney, *Electrochem. Commun.*, **8**, 1531 (2006).
10. C.S. Johnson, J.S. Kim, C. Lefief, N. Li, J.T. Vaughey and M.M. Thackeray, *Electrochem. Commun.*, **6**, 1085 (2004).
11. B.S. Jin, C.H. Doh, S.I. Moon, M.S. Yun, J.K. Jeong, H.D. Nam and H.G. Park, *J. Korean Electrochem. Soc.*, **7**, 4 (2004).
12. M.H. Lee, Y.J. Kang, S.T. Myung and Y.K. Sun, *Electrochim. Acta.*, **50**, 939 (2004).